Progress towards fundamental symmetry tests with nonlinear optical rotation

D. F. Kimball[1], D. Budker[1,2,†], D. S. English[1], C.-H. Li[1], A.-T. Nguyen[1], S. M. Rochester[1], A. Sushkov[1], V. V. Yashchuk[1], and M. Zolotorev[3]

[1] *Department of Physics, University of California at Berkeley, Berkeley, California 94720-7300*
[2] *Nuclear Science Division, Lawrence Berkeley National Laboratory, Berkeley, California 94720*
[3] *Center for Beam Physics, Lawrence Berkeley National Laboratory, Berkeley, California 94720*
[†] e-mail = budker@socrates.berkeley.edu

Abstract. Magneto-optical (Faraday) rotation is a process in which the plane of light polarization rotates as light propagates through a medium along the direction of a magnetic field. In atomic vapors where ground state atomic polarization relaxes very slowly (relaxation rates $\lesssim 1$ Hz), there arise ultranarrow, light-power-dependent (nonlinear) features in the magnetic field dependence of Faraday rotation. The shot-noise-limited sensitivity of a magnetometer based on nonlinear Faraday rotation can exceed 10^{-11} G/$\sqrt{\text{Hz}}$, corresponding to a sensitivity of $\sim 10^{-6}$ Hz/$\sqrt{\text{Hz}}$ to Zeeman sublevel shifts. Here we discuss recent progress in magnetometry based on nonlinear optical rotation and consider the application of these methods to searches for fundamental-symmetry-violating interactions.

INTRODUCTION

Professor Commins's heroic efforts in testing fundamental symmetries with atoms have inspired many of his students and "grandstudents" to follow in his footsteps. For example, a number of Professor Commins's former students are pursuing searches for the permanent electric dipole moment (EDM) of the electron in their own laboratories – Larry Hunter, who completed his first search for the electron EDM using optically-pumped cesium in a vapor cell filled with buffer gas [1] a full year before Professor Commins's initial EDM result [2]; Steven Chu, who has been working to develop an EDM experiment using optically-trapped cesium atoms [3]; David DeMille, who is pursuing an EDM measurement in metastable states of lead oxide [4]; and our own group, whose work is described in this paper. However, for the past decade no one has been able to match the sensitivity of Professor Commins's first electron EDM search using thallium [2] – let alone his two subsequent improvements [5, 6]!

In this contribution, we describe recent progress in our efforts to use nonlinear optical rotation for precision magnetometry. In addition, we discuss how the techniques developed for magnetometry can be applied to fundamental symmetry tests in atomic systems.

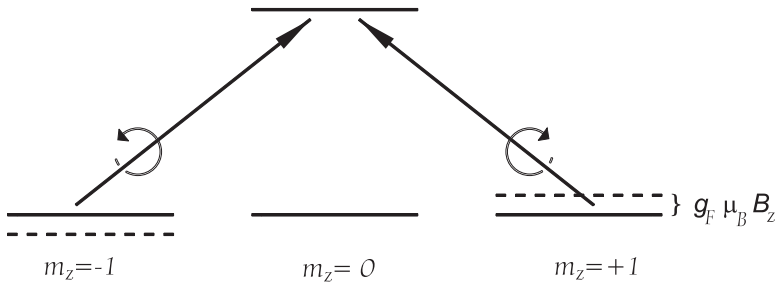

FIGURE 1. Energy level diagram for an $F = 1 \rightarrow F' = 0$ atomic transition.

LINEAR FARADAY ROTATION: THE MACALUSO-CORBINO EFFECT

When linearly-polarized light propagates through a medium immersed in a magnetic field, the plane of light polarization at the output is rotated; this effect was observed by Michael Faraday almost one hundred and fifty years ago [7]. In 1898, Italian physicists Macaluso and Corbino discovered that Faraday rotation was resonantly enhanced near atomic absorption lines [8].

The origin of this linear (light-power-independent) Faraday rotation (the Macaluso-Corbino effect) can be understood by considering, for example, an $F = 1 \rightarrow F' = 0$ atomic transition (Fig. 1); F and F' are the total angular momenta of the lower and upper state, respectively. Linearly polarized light incident on an atomic sample can be decomposed into left- (σ_+) and right- (σ_-) circularly polarized components. When a magnetic field B_z is applied to the sample along the direction of light propagation (the longitudinal direction, $\hat{z}$), the Zeeman shifts between adjacent magnetic sublevels ($= g_F \mu_B B_z$, where g_F is the Landé factor and μ_B is the Bohr magneton) cause the refractive indices for σ_+ and σ_- light to differ (circular birefringence). This, in turn, causes the circular components of the linearly-polarized light to change their relative phase as they propagate through the medium – leading to optical rotation (Fig. 2).

For the Doppler-free case with narrow-band light, the complex indices of refraction $n_\pm(\omega)$ for $\sigma_\pm$ light can be described by Lorentzian lineshape functions:

$$n_\pm(\omega) \approx 1 + 2\pi\chi_0 \cdot \left(\frac{\gamma_0}{2(\omega - \omega_0 \mp g_F \mu_B B_z) + i\gamma_0} \right), \tag{1}$$

where χ_0 is the amplitude of the linear optical susceptibility, ω is the light frequency, ω_0 is the resonant frequency of the atomic transition, and γ_0 is the natural linewidth. The difference between the refractive indices for σ_+ and σ_- light is given by:

$$n_+(\omega) - n_-(\omega) \approx -2\pi\chi_0 \cdot \frac{4 g_F \mu_B B_z / \gamma_0}{(2 g_F \mu_B B_z / \gamma_0)^2 + \left(1 - 2i\left(\frac{\omega - \omega_0}{\gamma_0}\right)\right)^2}. \tag{2}$$

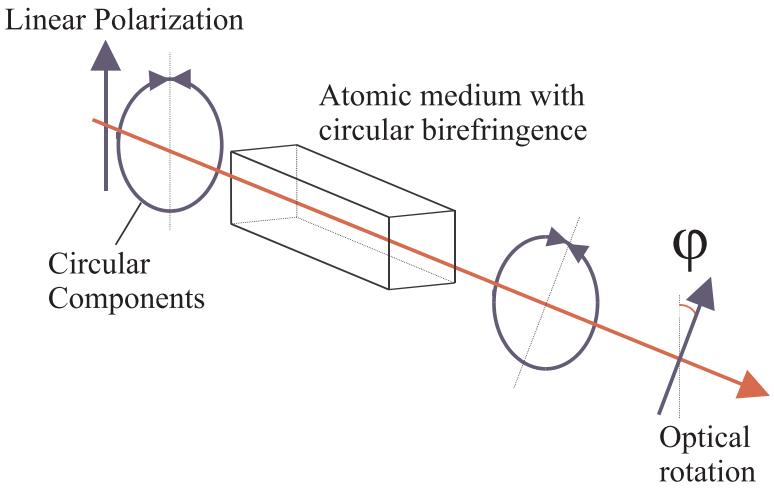

FIGURE 2. A medium possessing circular birefringence causes rotation of the plane of light polarization.

On resonance ($\omega = \omega_0$), this leads to optical rotation φ with a dispersively-shaped magnetic field dependence given by

$$\begin{aligned} \varphi &= \frac{\omega_0 \ell}{2c} \cdot \mathrm{Re}[n_+(\omega_0) - n_-(\omega_0)] \\ &\approx \frac{\ell}{2\ell_0} \cdot \frac{2g_F \mu_B B_z/\gamma_0}{1 + (2g_F \mu_B B_z/\gamma_0)^2}, \end{aligned} \tag{3}$$

where ℓ is the path length through the sample, c is the speed of light in vacuum, and $\ell_0 = (4\pi\chi_0\omega_0/c)^{-1}$ is the unsaturated absorption length on resonance. For media where the linewidth of the atomic transition is primarily determined by Doppler broadening, the indices of refraction are described by Gaussian functions, and thus optical rotation on resonance is given by

$$\varphi \approx \frac{\ell}{2\ell_0} \cdot \frac{2g_F \mu_B B_z}{\Gamma_D} \cdot e^{-(g_F \mu_B B_z/\Gamma_D)^2}, \tag{4}$$

where Γ_D is the Doppler width.

Any physical mechanism that causes a relative shift of the energies of the $\pm m_z$ sublevels will lead to optical rotation. For example, in Refs. [9, 10] it was proposed that the analog of linear Faraday rotation in the presence of a longitudinal electric field could be used to search for an EDM.

The sensitivity $\delta\Delta$ of an optical rotation measurement to a shift of the Zeeman sublevels Δ (where in the case of magneto-optical rotation, Δ is the Zeeman shift) is

given by:

$$\delta\Delta = \left(\frac{\partial\varphi}{\partial\Delta}\right)^{-1}\delta\varphi, \tag{5}$$

where $\delta\varphi$ is the sensitivity to light polarization rotation (measured in, e.g., rad$/\sqrt{\text{Hz}}$) and $\partial\varphi/\partial\Delta$ is the slope of the optical rotation with respect to the energy shift Δ. The shot-noise limit of $\delta\varphi$ is inversely proportional to the square root of the light power transmitted through the atomic vapor [11]. For an atomic transition whose linewidth is dominated by Doppler broadening, we find from Eqs. (4) and (5) that for small Δ ($\Delta \ll \Gamma_D$)

$$\delta\Delta \approx e^{\ell/2\ell_0}\cdot\sqrt{\frac{\pi}{P_0}}\cdot\frac{\ell_0}{\ell}\cdot\Gamma_D, \tag{6}$$

where P_0 is the incident light flux in photons per second (we ignore factors of order unity related to the polarimetry method). Note that the same result is obtained for Doppler-free media from Eq. (3), except that Γ_D is replaced by γ_0.

One can also see from Eq. (6) that the optimal sensitivity is achieved when

$$\frac{\partial}{\partial\ell}\left(\frac{e^{\ell/2\ell_0}}{\ell}\right) = \frac{e^{\ell/2\ell_0}}{\ell}\left(\frac{1}{2\ell_0}-\frac{1}{\ell}\right) = 0, \tag{7}$$

or when $\ell = 2\ell_0$.

It is also important to note that at high light powers, saturation effects become important, and therefore the sensitivity cannot be arbitrarily improved by increasing P_0.

COHERENCE EFFECTS IN NONLINEAR FARADAY ROTATION

At sufficiently high light powers, there arise light-power-dependent (nonlinear) features in the magnetic field dependence of Faraday rotation which are related to optical pumping (for reviews, see, e.g., Refs. [12, 13]). Such nonlinear magneto-optical rotation (NMOR) can arise due to the formation of Bennett structures in the atomic velocity distribution [14] and (for transitions involving states with $F > 1/2$) due to the evolution of optically-pumped atomic polarization (see, e.g., Ref. [15]). Figure 3 shows a density matrix calculation [16, 17] of the magnetic field dependence of Faraday rotation for the case of the 571 nm line ($1 \rightarrow 0$) in samarium (studied experimentally in Ref. [15]).

In Doppler-broadened media, the linear effect has a width determined by Γ_D, the Bennett-structure-related effect has a width determined by γ_0 [17], and NMOR due to the evolution of optically-pumped, ground state polarization has a width determined by the relaxation rate of coherences between ground state Zeeman sublevels γ_{rel}. γ_{rel} can be made very small by employing buffer gases or using vapor cells with anti-relaxation wall coatings. As can be seen from Fig. 3, nonlinear effects greatly enhance the small-field optical rotation.

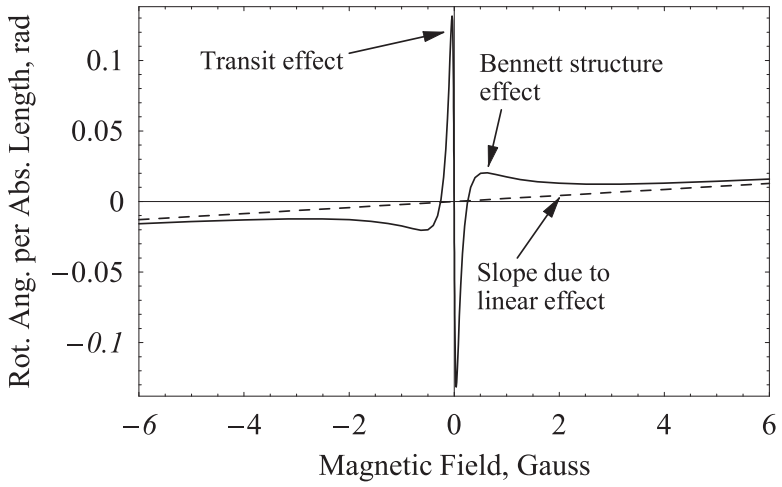

FIGURE 3. Density matrix calculation of light polarization rotation as a function of longitudinal magnetic field for the case of the samarium 571 nm line, under the conditions of the experiment described in Ref. [15]. Under these conditions, $\gamma_{\rm rel}$ is determined by the transit rate of atoms through the laser beam (diameter $\sim$ 1 mm), hence the coherence effect in this case is termed the "transit effect."

Low light power: linear dichroism

First we consider relatively low light powers for which the optical pumping saturation parameter $\kappa \ll 1$, where

$$\kappa = \frac{d^2 E_0^2}{\gamma_0 \gamma_{\rm rel}}, \tag{8}$$

d is the transition dipole moment, and E_0 is the amplitude of the optical electric field. Under these conditions, NMOR related to the coherence effects is due to precession of optically-pumped atomic alignment (see, e.g., Refs. [18, 19, 20] and references therein).

Consider a closed $F = 1 \rightarrow F' = 0$ transition (Fig. 4). Resonant, linearly polarized (along x) light optically pumps the atomic sample into dark states (the $m_x = \pm 1$ states) – the vapor thus acquires an axis of linear dichroism (it is transparent to x-polarized light and strongly absorbs y-polarized light). The $\hat{z}$-directed magnetic field causes the atomic alignment to precess (Fig. 5). Since the axis of linear dichroism is no longer along the light polarization, the polarization plane of light rotates as the light propagates through the medium.

In a magnetic field, the optically-pumped atomic polarization precesses at the Larmor frequency $g_F \mu_B B_z$ and relaxes at a rate $\gamma_{\rm rel}$. The aligned atoms can be treated as linear polarizers which rotate the light polarization by an angle $d\varphi \propto \sin(2 g_F \mu_B B_z)$. On resonance for an optically thin medium ($\ell/\ell_0 \ll 1$), the overall rotation φ produced by the entire collection of atoms is given by

$$\begin{aligned} \varphi &= \eta \cdot \frac{\ell}{2\ell_0} \frac{\int_{t=0}^{\infty} dt\; e^{-\gamma_{\rm rel} t} \sin(2 g_F \mu_B B_z t)}{\int_{t=0}^{\infty} dt\; e^{-\gamma_{\rm rel} t}} \\ &= \eta \cdot \frac{\ell}{2\ell_0} \frac{2 g_F \mu_B B_z / \gamma_{\rm rel}}{1 + (2 g_F \mu_B B_z / \gamma_{\rm rel})^2}, \end{aligned} \tag{9}$$

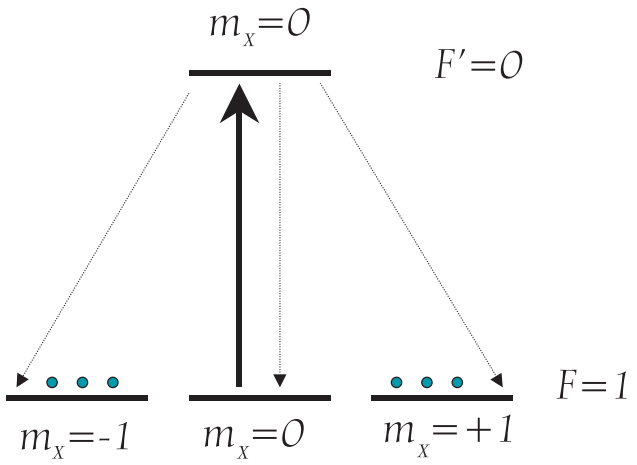

FIGURE 4. For an $F = 1 \rightarrow F' = 0$ transition, optical pumping by linearly polarized light along x creates an atomic ensemble consisting of an incoherent mixture of atoms in the $m_x = \pm 1$ states. Dots represent the population of the different ground state sublevels.

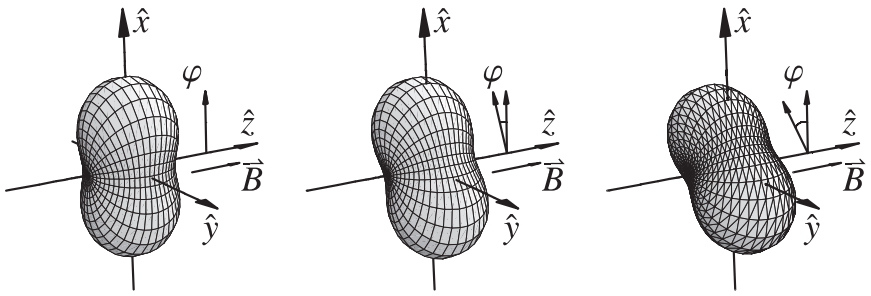

FIGURE 5. Sequence showing the evolution of optically-pumped, ground state atomic alignment in a longitudinal magnetic field for an $F = 1 \rightarrow F' = 0$ transition at low light powers, time proceeds from left to right. The distance from the surface to the origin represents the probability of finding the projection $m = F$ along the radial direction (see Ref. [25] for a detailed description of this method of representing atomic polarization). In the first plot, the atoms have been optically pumped into an aligned state by x-polarized light (they have been pumped out of the "bright" state, which interacts with the light field, into "dark" states which do not). Note that, just as in Fig. 4, the highest probability of finding $m = F$ is obtained for $\pm\hat{x}$. The magnetic field along $\hat{z}$ creates a torque on the polarized atoms, causing the alignment to precess (second and third plots). This rotates the medium's axis of linear dichroism, which is observed as a rotation of the polarization of transmitted light by an angle φ with respect to the initial light polarization.

where t is the time between pumping and probing for a given atom, and $\eta < 1$ is a factor that accounts for the efficiency of optical pumping and probing in the system.

The sensitivity of a measurement of optical rotation produced by the low-light-power coherence effect to small shifts of the Zeeman sublevels ($\Delta \ll \gamma_{\rm rel}$) is given, in analogy with Eq. (6), by

$$\delta\Delta \approx \frac{1}{\eta} \cdot e^{\ell/2\ell_0} \sqrt{\frac{\pi}{P_0}} \cdot \frac{\ell_0}{\ell} \cdot \gamma_{\rm rel}. \tag{10}$$

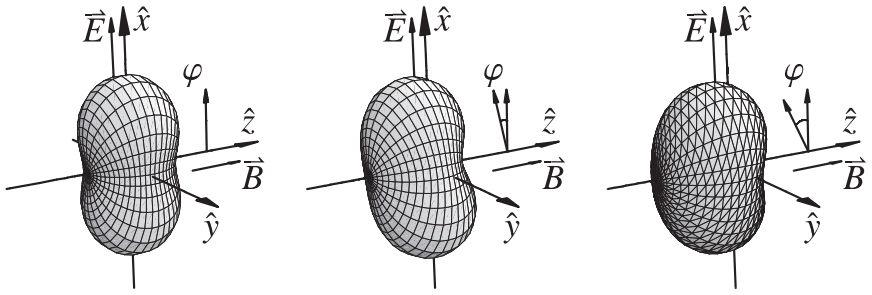

FIGURE 6. Sequence showing the evolution of optically-pumped, ground state atomic alignment in a longitudinal magnetic field for an $F = 1 \rightarrow F' = 0$ transition for high light powers, time proceeds from left to right. In the first plot, the atoms have been polarized along the axis of light polarization as in Fig. 5. If the atomic alignment is parallel to the optical electric field, the ac Stark shifts have no effect on the atomic polarization – they merely shift the energies of the bright and dark states relative to each other. However, when the magnetic field along $\hat{z}$ causes the alignment to precess, the atoms evolve into a superposition of the bright and dark states (which have different energies due to the ac Stark shifts), so optical-electric-field-induced quantum beats occur. These quantum beats produce atomic orientation along $\hat{z}$, which appears in the second plot and grows in the third plot, causing optical rotation due to circular birefringence.

Once again, as in the case of linear optical rotation, the maximum sensitivity is obtained for $\ell = 2\ell_0$. It is also important to note that for $\kappa \gtrsim 1$ saturation effects become important and a different physical mechanism can play an important role in optical rotation (see below). The maximum P_0 that can be realized without loss of sensitivity corresponds to $\kappa \sim 1$, so from Eqs. (8) and (10), we find that $\delta\Delta \propto \sqrt{\gamma_{\rm rel}}$.

As will be discussed below, in paraffin-coated alkali vapor cells, $\gamma_{\rm rel}$ can reach $\sim 2\pi \times 1$ Hz [21, 22, 23, 20]. Thus the coherence effects enhance the sensitivity of a measurement of optical rotation to level shifts by several orders of magnitude (compared to linear optical rotation)! In fact, our measurements of NMOR in paraffin-coated alkali vapor cells [20, 24, 26] (described below) indicate that the sensitivity of an NMOR-based magnetometer can compete with current state-of-the-art optical pumping magnetometers [27] and superconducting quantum interference device (SQUID) magnetometers [28].

High light power: alignment-to-orientation conversion

At relatively high light powers, where $\kappa \gtrsim 1$ (Eq. (8)), a different physical mechanism can become important for NMOR [29]. Under such conditions, the evolution of the optically-pumped ground state atomic alignment involves both Larmor precession due to the magnetic field and Stark beats due to the presence of the strong optical electric field. This combined action of the magnetic and optical electric fields causes atoms to acquire orientation along the direction of the magnetic field (alignment-to-orientation conversion (AOC) [30, 31, 32, 33, 34]). A sample oriented along the direction of light propagation has a difference in the populations of the $\pm m_z$ sublevels. An oriented sample causes optical rotation due to circular birefringence, since the refractive indices for σ_+ and σ_- light are different. The evolution of atomic polarization for the NMOR coherence

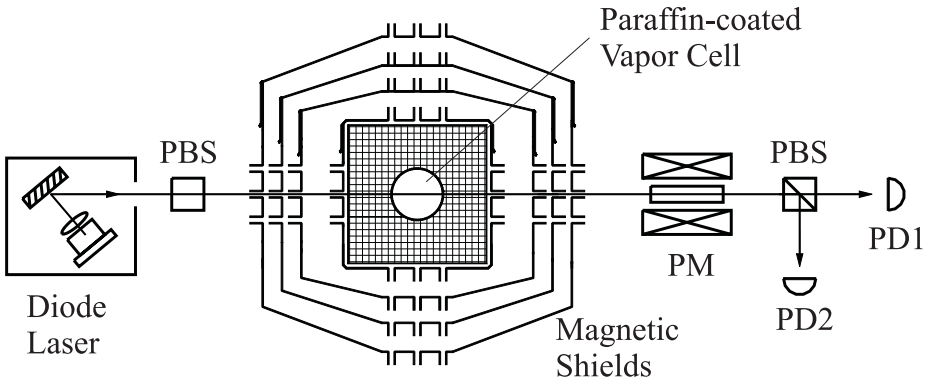

FIGURE 7. Schematic diagram of the apparatus used for nonlinear Faraday rotation measurements. PBS = polarizing beamplitter; PM = polarization modulator; PD1,2 = photodiodes.

effect for an $F = 1 \rightarrow F' = 0$ transition at high light power is illustrated in Fig. 6.

The atomic orientation produced by AOC is proportional to $\vec{d}_{\rm ind} \times \vec{E}_0$, where $\vec{d}_{\rm ind}$ is the induced electric dipole moment caused by the interaction of atoms (whose optically pumped alignment has precessed in the magnetic field) with the optical electric field $\vec{E}_0$. The quantity $\vec{d}_{\rm ind} \times \vec{E}_0$ is proportional to the ac Stark shift, which has an antisymmetric dependence on detuning of the light from the atomic resonance. Thus, net orientation in the cell can only be produced when light is detuned from resonance.

EXPERIMENTS WITH ANTI-RELAXATION COATED CELLS

As discussed above, the sensitivity of nonlinear optical rotation to interactions that shift the energies of the Zeeman sublevels can be considerably enhanced by reducing the relaxation rate of atomic polarization. In our experiments [20, 24, 26], we obtain ultranarrow NMOR resonances ($\gamma_{\rm rel} \approx 2\pi \times 1$ Hz) by using evacuated alkali vapor cells with high quality paraffin coating [27]. In such cells, atoms can undergo many thousand wall collisions without depolarizing.

Experimental Apparatus

A schematic diagram of the experimental apparatus used in the present measurements is shown in Fig. 7, and is essentially the same as that described in Refs. [20, 24, 26]. The alkali atoms are contained in buffer-gas-free, paraffin-coated cells. The cells are made by our collaborators in St. Petersburg, Russia (E. B. Alexandrov and M. V. Balabas), and the cell preparation procedure is described in Refs. [35, 36].

A cell is placed inside a four-layer magnetic shield with a shielding factor of 10^6 in all directions [24]. Three mutually perpendicular magnetic coils allow for compensation of residual magnetic fields inside the shields to a level of 0.1 μG (averaged over the cell volume) and application of arbitrarily-directed, well-controlled magnetic fields to the vapor

cell. The gradients inside the shields have been measured by NMOR using a spherical (10 cm diameter) paraffin-coated cell containing ^{87}Rb on a movable mount, and the gradients were found to be ≈ 5 μG/cm and essentially independent of temperature (they changed by $\lesssim 1$ μG/cm over a 10°C variation in cell/shield temperature). Since, under typical conditions, atoms undergo $\sim 10^3$ wall collisions between pumping and probing, the contribution of the gradients to $\gamma_{\rm rel}$ is significantly suppressed due to motional narrowing. Estimates and measurements of "relaxation in the dark" [37] as a function of leading magnetic field indicate that gradients contribute no more than $\sim 2\pi \times 0.5$ Hz to $\gamma_{\rm rel}$.

We use tunable extended cavity diode lasers to produce light at 795 nm for the Rb D1 line ($^2S_{1/2} \rightarrow {}^2P_{1/2}$), 780 nm for the Rb D2 line ($^2S_{1/2} \rightarrow {}^2P_{3/2}$), and 852 nm for the Cs D2 line ($^2S_{1/2} \rightarrow {}^2P_{3/2}$). NMOR signals are detected using the technique of polarization-modulation polarimetry (see, e.g., Ref. [38]). After passing through the coated Rb vapor cell, light goes through a Faraday rotator which modulates the direction of linear polarization at a frequency of $\Omega_m = 2\pi \times 1$ kHz with a 5 mrad amplitude. The polarization of the light is subsequently analyzed with a polarizing beamsplitter with one of the transmission axes aligned with the initial light polarization. The signal from the photodiode PD1 (which detects light from the dark port of the polarizing beamsplitter) at the first harmonic of Ω_m is measured with a lock-in amplifier. Transmitted light intensity is the sum of the light detected in the bright channel (PD2) and the dark channel (PD1) of the analyzer. The ratio of the first harmonic signal from PD1 to the transmitted light intensity is a measure of the optical rotation angle (see, e.g., [38]).

Sensitivity of nonlinear optical rotation measurements to level shifts

Figure 8 shows optical rotation as a function of magnetic field for light resonant with the ^{85}Rb D2 $F = 3 \rightarrow F'$ transition (this data was taken using a 10 cm diameter spherical cell). As discussed above, the width of this dispersively-shaped feature is determined by the relaxation rate of atomic polarization in the cell. The data shown in Fig. 8 are fit by Eq. (9), and for this particular data set we find that $\gamma_{\rm rel} \approx 2\pi \times 0.9$ Hz. The slope of the the optical rotation with respect to B_z in the linear region near $B_z = 0$ determines the shot-noise-limited sensitivity of NMOR to level shifts (Eq. (5)).

We have studied the sensitivity of an NMOR-based ^{85}Rb magnetometer as a function of light power and light frequency [26], and found that the optimum sensitivity occurred at a light intensity of ≈ 5 mW/cm^2 tuned ≈ 400 MHz to the high-frequency side of the $F = 3$ hyperfine component of the ^{85}Rb D2 line. Similar sensitivity is obtained for the ^{85}Rb D1 line at a light intensity of ≈ 1 mW/cm^2 tuned ≈ 600 MHz to the low-frequency side of the $F = 3$ hyperfine component. The optimum sensitivity corresponds to a shot-noise-limited sensitivity to Zeeman sublevel shifts of $\sim 10^{-6}$ Hz/$\sqrt{\rm Hz}$. It is interesting to note that this sensitivity is close to the fundamental shot-noise limit for an ideal setup with the given number of atoms in the vapor cell ($\sim 10^{12}$ at room temperature ≈ 20 °C) and rate of ground state relaxation ($\sim 2\pi \times 1$ Hz). Thus under optimum conditions, the shot noise due to photons is about the same as the shot noise

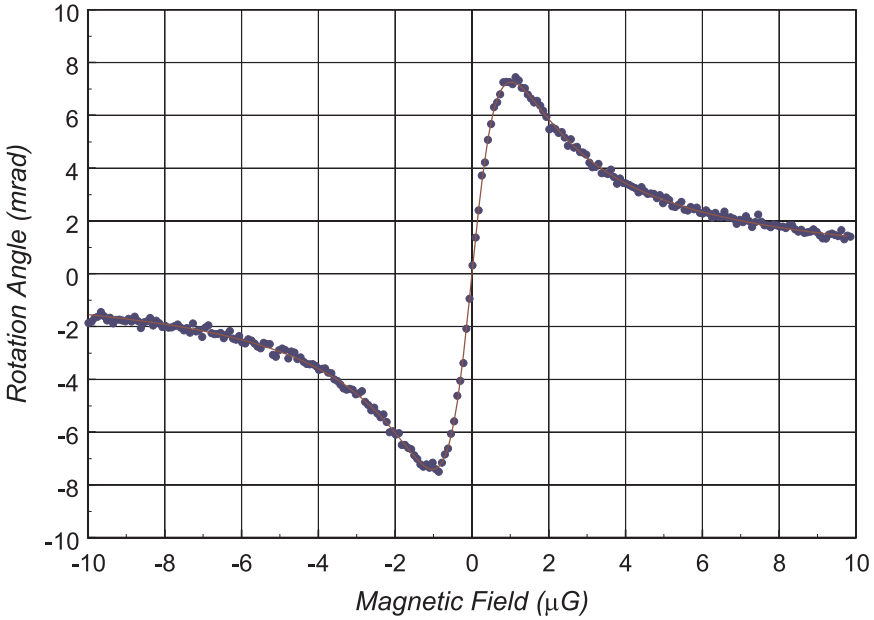

FIGURE 8. Magnetic field dependence of nonlinear Faraday rotation in a paraffin-coated cell (diameter $\approx$ 10 cm). Laser light is tuned to the high frequency slope of the ^{85}Rb D2 $F = 3 \rightarrow F'$ transition where maximum rotation occurs, light intensity $\approx 50\,\mu\mathrm{W/cm^2}$, beam diameter $\approx$ 2 mm. The temperature of the cell was $\approx 19^{\circ}$C and the vapor density of ^{85}Rb was $\approx 4 \times 10^9$ cm^{-3}. Dots are experimental data and the solid line is a fit to Eq. (9).

due to atoms. The ability of nonlinear optical rotation to reach the fundamental shot-noise limit for an ideal experiment demonstrates the great potential of this technique for precision measurements.

Light-induced atomic desorption of Rb and Cs from paraffin coating

An interesting feature of anti-relaxation coated cells is that upon illumination by nonresonant light, the alkali vapor density inside the cells increases. For example, when a cylindrical cell (diameter $\approx$ 5 cm, height $\approx$ 2 cm) containing both Rb and Cs was exposed to fluorescent room light, the vapor densities of both Rb and Cs increased by a factor of ~ 2. Since exposure to the light caused no measurable change in the cell temperature ($< 0.1^{\circ}$C), the increase in atomic density did not result from heating of the vapor cell. When the lights were turned off, the atomic density in the cell returned to its original value after a few minutes.

This effect is caused by light-induced desorption of atoms from the paraffin coating, which is discussed in more detail in Ref. [36]. Such nonthermal, light-induced desorption of atoms has previously been observed from a wide variety of materials: sapphire surfaces [39], silane-coated glass [40, 41, 42, 43, 44], and even from a superfluid ^{4}He film [45]. The effect depends on the wavelength and power of the desorbing light, and in most cases appears to involve both light-induced desorption of atoms from the surface of the material and light-assisted diffusion of atoms inside the material.

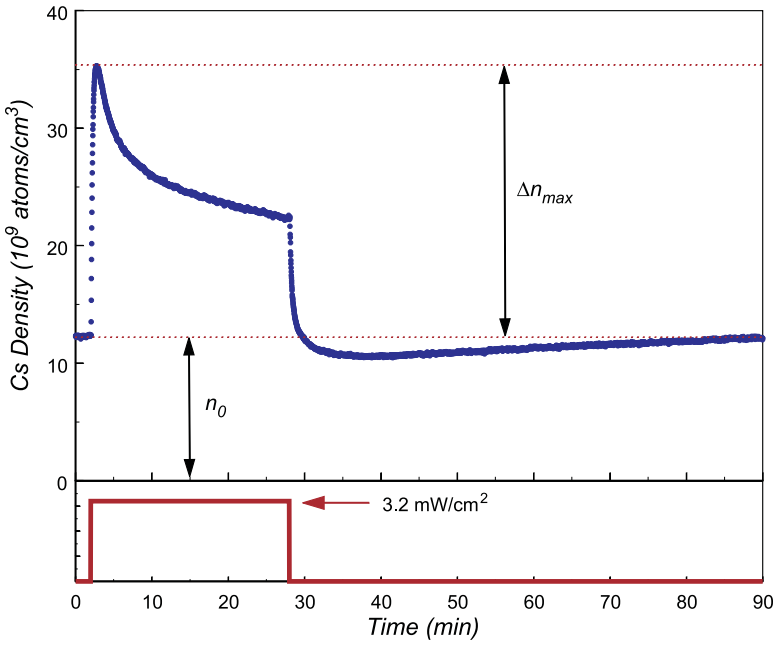

FIGURE 9. Upper plot shows Cs density as a function of time. The Cs density was measured by monitoring the transmission of a weak probe beam (intensity $\approx 10\,\mu\mathrm{W/cm^2}$, diameter ≈ 2 mm) through the alkali vapor cell. n_0 is the initial density before exposure to light, Δn_{max} is the maximum increase in density. Lower plot shows intensity of desorbing light as a function of time, beam diameter ≈ 6.4 cm^2.

Figure 9 shows the time dependence of the Cs density before, during, and after the cylindrical cell was exposed to 546-nm light from an Ar^+-pumped dye laser (Coherent CR-699 using Rhodamine 560). Measurements of the time and light power dependence of atomic desorption were used to characterize properties of the paraffin-coated cells, such as the adsorption probability, adsorption energy, and the surface density of adsorbed atoms.

SEARCH FOR THE PERMANENT ELECTRIC DIPOLE MOMENT OF THE ELECTRON

As was pointed out in Refs. [9, 10], if an atom possesses a permanent electric dipole moment (EDM, for reviews, see e.g., [46, 47]), a longitudinal electric field will cause an atomic vapor to become optically active, leading to rotation of the plane of light polarization – the analog of Faraday rotation. In Ref. [48], it was demonstrated that nonlinear optical rotation is significantly more sensitive than linear optical rotation to the EDM of an atom or molecule.

We are presently investigating the possibility of performing a search for the electron EDM d_e using nonlinear optical rotation. For this experiment, a longitudinal electric field (along $\hat{z}$) would be applied to a paraffin-coated vapor cell containing both Rb and Cs. Rb, whose enhancement factor for the electron EDM is much smaller than that of Cs, would be used as a "co-magnetometer." If Cs possessed a permanent dipole moment

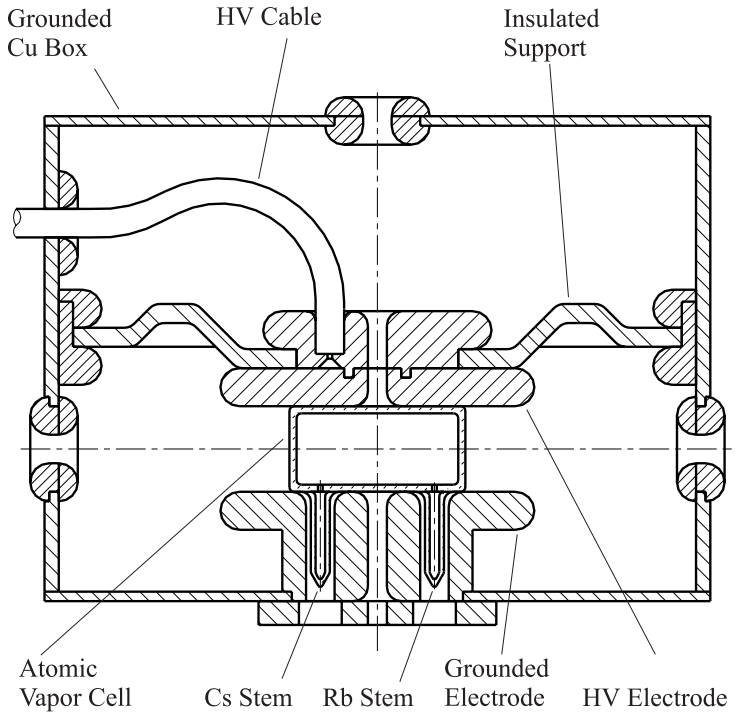

FIGURE 10. High-voltage electrode assembly for application of electric fields to paraffin-coated vapor cell. Outer shell and bottom plate (made of copper) are grounded, high voltage is applied to the upper plate. Windows allow laser beam access to the antirelaxation-coated vapor cell in three orthogonal directions. Metal corners are rounded to prevent discharges.

$\vec{d}$, the atomic polarization would precess in the longitudinal electric field $\vec{E}$ because of the $\vec{d} \times \vec{E}$ torque. The change in atomic polarization would in turn modify the light polarization, just as in the case of NMOR in a magnetic field.

There were, in fact, a number of experimental searches for d_e [49, 50, 51] carried out at the University of Washington using alkali atoms contained in paraffin-coated cells in the 1960's and early 1970's that set a limit of $d_e < 1.6 \times 10^{-23}$ e $\cdot$ cm [51]. In these experiments, the atoms were optically pumped into oriented states by circularly-polarized light propagating at 45° to the direction of applied electric ($\approx \pm 300$ V/cm) and magnetic fields (≈ 27 mG). An rf-field was applied perpendicularly to the electric and magnetic fields, which, in conjunction with the pump light, produced an oriented atomic sample that precessed about the fields (this is the configuration of a Dehmelt oscillator [52]). The precession frequency was measured by monitoring the modulation of light absorption. To look for the effect of an EDM, the modulation frequency of the transmitted light power was measured for $\pm$ electric field values. The statistical sensitivity of these experiments was limited by photon shot noise, while the primary systematic effect limiting the experiments was a change in the cell properties when the electric fields were applied.

For the proposed EDM experiment using nonlinear optical rotation, we expect to achieve significantly better statistical sensitivity [24, 26] than the previous experiments in paraffin-coated cells [49, 50, 51]. Our estimated shot-noise-limited sensitivity to d_e

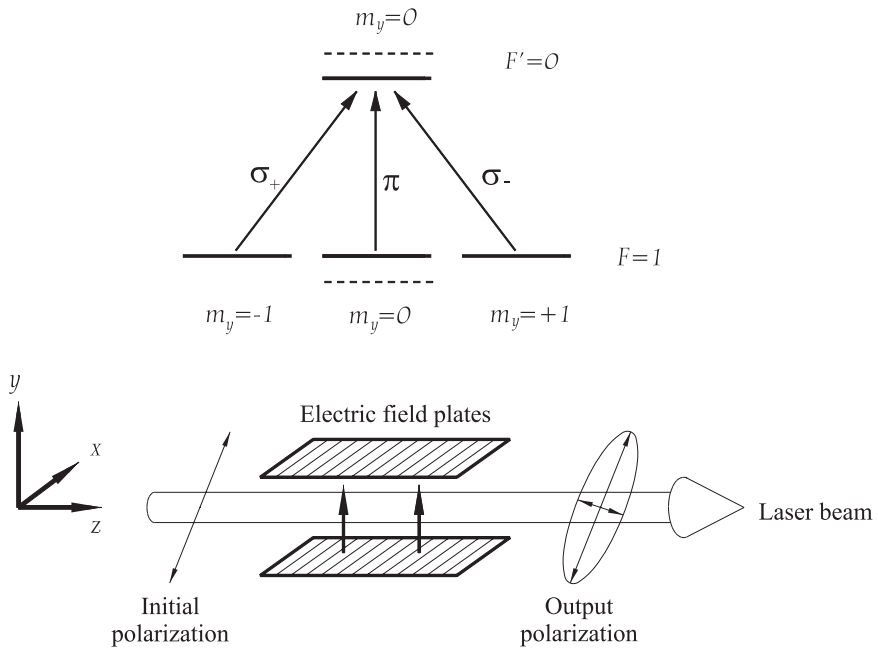

FIGURE 11. Schematic diagram of NEOE measurement for an $F = 1 \rightarrow F' = 0$ transition. In the presence of an electric field along the quantization axis ($\hat{y}$), the $m_y = 0$ Zeeman sublevels are shifted by the Stark effect (dashed lines). As a result there arises a difference in the resonance frequencies for y-polarized (π) and x-polarized light (which can be represented as a superposition of $\sigma_{\pm}$ light). As the light propagates through the atomic medium in the presence of the electric field, the initially linearly-polarized light develops ellipticity.

is $\approx 10^{-26}$ e $\cdot$ cm$/\sqrt{\text{Hz}}$ (for a 10 kV/cm electric field and taking into account the EDM enhancement factor of ≈ 120 for Cs [53, 54, 55, 56]). This statistical sensitivity should enable a nonlinear-optical-rotation-based EDM search to compete with the best present limits on d_e from measurements in Cs [1] and even in Tl [6].

However, in order to reach this projected sensitivity, there are several problems that must be overcome. The first is a change in the atomic density when electric fields are applied to the cell. The second is a coupling of the atomic polarizations of Cs and Rb via spin-exchange collisions, which would prevent Rb from functioning as an independent co-magnetometer. These effects are discussed in more detail in the following sections.

Application of electric fields to paraffin-coated cells and measurements of nonlinear electro-optical effects

The high-voltage electrode assembly used in our present measurements is shown in Fig. 10. The electrode assembly, containing a cylindrical, paraffin-coated Rb-Cs cell (diameter ≈ 5 cm, height ≈ 2 cm), is placed inside the 3D coils and magnetic shields shown in Fig. 7.

We have performed measurements of the electric field inside the cell using a nonlinear electro-optical effect induced by Stark shifts [57]. This effect can be understood by

considering, e.g., an isolated $F = 1 \rightarrow F' = 0$ transition, where we choose the quantization axis along the $\hat{y}$ direction (Fig. 11). Light that is initially linearly polarized at 45° to the x-axis can be decomposed into x-polarized (a superposition of $\sigma_{\pm}$) and y-polarized (π) light. If a $\hat{y}$-directed electric field is applied to the sample, the quadratic Stark effect causes a relative shift in the resonance frequencies for x- and y-polarized light, resulting in a difference in the corresponding refractive indices. A linear electro-optical effect arises in this case since as near-resonant light propagates through the atomic medium, y-polarized light changes its phase relative to the x-polarized light. Thus the transmitted light acquires elliptical polarization due to linear birefringence.[1] Like in the case of NMOR, there arise nonlinear electro-optic effects due to the formation of Bennett structures in the atomic velocity distribution for atoms in particular ground state sublevels [17] and optically-pumped ground state coherences. These effects can considerably enhance the induced ellipticity with respect to the linear case.

To measure the nonlinear electro-optical effects, light resonant with the Rb D2 transition is directed through the cell perpendicular to the direction of the applied electric field. Before entering the cell, the light passes through a linear polarizer oriented at 45° to the direction of the applied electric field (Fig. 11). After the light passes through the cell, the degree of ellipticity ε is determined by a circular analyzer consisting of a quarter-wave plate with fast axis along y and a polarizing beamsplitter.

Figure 12 shows the spectrum of induced ellipticity for the ^{85}Rb D2 line when an electric field of ~ 5 kV/cm is applied to the cell. The light power is $\approx 3.5\ \mu$W and the laser beam diameter is ≈ 1 mm. The density of ^{85}Rb is $\approx 10^9$ atoms/cm^3, somewhat lower than the saturated density at room temperature (20°C) [59]. Note that the quadratic Stark shifts are larger in the upper state of the D2 transition, since the total electronic angular momentum J is $1/2$ for the lower state (so ground state Stark shifts arise only due to the hyperfine interaction). Density matrix calculations [16, 17] indicate that the measured ellipticity in Fig. 12 is primarily due to Bennett structures, and not coherence effects or the linear electro-optical effect.[2] These data show that atoms inside the vapor cell are experiencing close to the full 5 kV/cm electric field that is applied.

During the electric field measurements, we observed a dramatic change in the alkali vapor density when the electric field polarity was switched. Figure 13 shows the Cs vapor density and applied electric field as a function of time. If the electric field amplitude is changed without changing the polarity, there is no significant change in alkali vapor density. This effect is probably similar to the electric-field-related degradation of paraffin coated cells observed in the Seattle EDM experiments [49, 50, 51].[3] One characteristic

---

[1] The major axis of the ellipse is also rotated with respect to the initial light polarization due to linear dichroism. However, due to the different spectral lineshapes of rotation and ellipticity, Doppler broadening suppresses optical rotation relative to ellipticity by a factor of Γ_D/γ_0.

[2] The present density matrix calculation ignores the fact that the atoms can undergo collisions with the cell walls without depolarizing, which can affect the magnitude of the induced ellipticity by a factor estimated to be of order unity.

[3] It is interesting to note that similar behaviour has been observed for ^{199}Hg atoms cohabiting an ultracold neutron storage container (with quartz walls and teflon-coated electrodes) in the neutron EDM experiment at the Institut Laue-Langevin (ILL) [58]. In the ILL experiment, both the Hg density and atomic polarization relaxation rate changed when the polarity of the electric field was reversed.

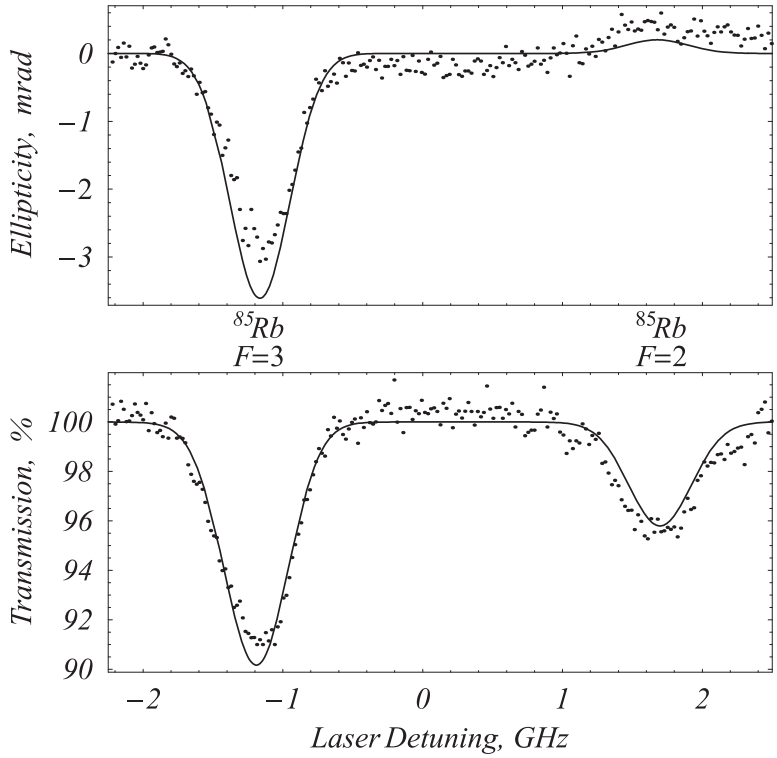

FIGURE 12. Upper plot compares a measurement of electric-field-induced ellipticity for the ^{85}Rb D2 line to a density matrix calculation. Lower plot shows the experimental and theoretical transmission spectra.

of this effect is the very slow recovery rate of the alkali vapor density after switching the electric field ($\sim$ 20 min). This time scale is similar to the recovery times observed in light-induced desorption measurements (Fig. 9) when the paraffin surface has been depleted of adsorbed alkali atoms. Also, we have found that the vapor density recovers more quickly when the stems (containing solid samples of Cs and Rb) are heated. These characteristics suggest that the electric field may be somehow depleting the paraffin of adsorbed atoms – thus changing the relative fluxes of atoms being adsorbed and desorbed from the paraffin coating. This effect is presently under investigation, and the results will be reported elsewhere.

NMOR with frequency-modulated light

An essential feature of the proposed EDM search using nonlinear optical rotation is the use of Rb as a "co-magnetometer," so in effect the experiment will measure a difference in the linear Stark shifts for Rb and Cs. In order for the Cs and Rb atoms to act independently, "locking" of the Cs polarization to the Rb polarization via spin-exchange collisions must be avoided.

The transfer of longitudinal (along the magnetic field direction) spin polarizations

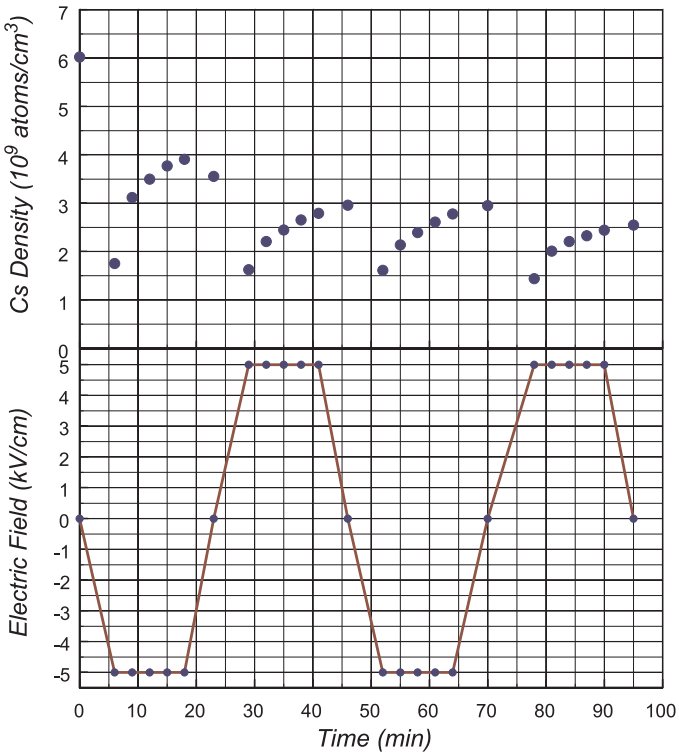

FIGURE 13. Upper plot shows Cs vapor density in a paraffin-coated cell as a function of time, lower plot shows applied electric field.

between species via spin-exchange collisions can be quite efficient: the Rb-Cs spin-exchange cross section is $\approx 2 \times 10^{-14}$ cm^2 [60]. Transverse spin polarization is more difficult to transfer because the transverse spin components of Cs and Rb dephase due to the difference between their Larmor frequencies [61, 62]. Nonetheless, at small magnetic fields (where the difference between the Cs and Rb Larmor frequencies is less than the relaxation rate of atomic polarization), efficient polarization transfer can occur. In the case where only transverse spin polarization is present, "locking" of the Cs polarization to the Rb polarization can be avoided by applying a bias magnetic field. However, using the NMOR techniques previously discussed, measurements can only be performed in small magnetic fields ($B_z < \gamma_{\rm rel}/g_F\mu_B$).

Recently, we have developed a technique that can extend the dynamic range of an NMOR-based magnetometer to the Earth field range [63]. In this setup (Fig. 14), light polarization modulation (see Fig. 7) is replaced by frequency modulation of the laser, and the time-dependent optical rotation is measured at the first harmonic of the light modulation frequency Ω_m (FM NMOR). The frequency modulation affects both optical pumping and probing of atomic polarization, causing resonances to arise in the magnetic field dependence when Ω_m coincides with twice the Larmor frequency $2\Omega_L$. Additional resonances can be observed at higher harmonics, for example a resonance arises at the second harmonic of Ω_m when $\Omega_m = \Omega_L$.

The FM NMOR signals at the first harmonic of Ω_m as a function of longitudinal magnetic field are shown in Fig. 15. For these measurements, a spherical paraffin-coated

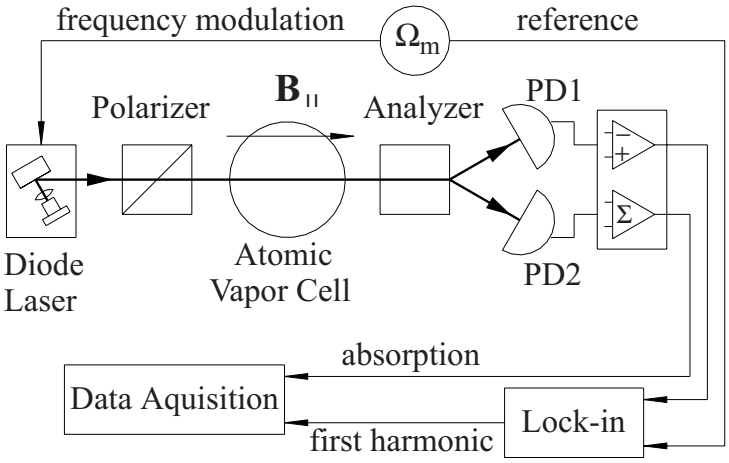

FIGURE 14. Schematic diagram for measurement of NMOR with frequency-modulated light. Paraffin-coated cell containing ^{87}Rb is placed between a polarizer and an analyzer oriented at $\approx 45^{\circ}$ with respect to each other. For the present measurements, the laser frequency is modulated with a piezo actuator in the diode laser.

cell (diameter ≈ 10 cm) containing ^{87}Rb is employed. The laser frequency is modulated at $\Omega_m = 2\pi \times 1$ kHz with modulation amplitude $\Delta\omega = 2\pi \times 220$ MHz. The laser is tuned to the low-frequency slope of the $F = 2 \rightarrow F' = 1$ component of the D1 resonance where the signal at the first harmonic is maximal.

For low light powers, where optical pumping primarily produces atomic alignment (see Figs. 4 and 5), the origins of the FM NMOR resonances can be understood as follows. Resonances at the first harmonic of Ω_m occur at $\Omega_L = 0$ and when the modulation frequency of the pumping and probing light corresponds to $2\Omega_L$. As the laser frequency is modulated, the optical pumping rate changes depending on the instantaneous detuning of the laser from the atomic transition, given by $\omega(t) - \omega_0$ where $\omega(t) = \omega_l + \Delta\omega \cdot \sin(\Omega_m t)$ (ω_l is the central frequency of the laser). For a spectrally-isolated, Doppler-broadened transition, the time-dependent pumping (and probing) rates are

$$\propto e^{-(\frac{\omega(t)-\omega_0}{\Gamma_D})^2}.$$

When the pumping rate is synchronized with the precession of atomic polarization, a resonance occurs and the atomic medium is pumped into an aligned state whose axis rotates at Ω_L. The optical properties of the medium are modulated at $2\Omega_L$, due to the symmetry of atomic alignment. Since the probability for probing is modulated, optical rotation due to the average axis of atomic alignment being at an angle to the light polarization (which has a resonant character) results in the zero-field resonance.

If alignment-to-orientation conversion occurs (see Fig. 6 and Ref. [29]), a longitudinal spin polarization arises, and spin-exchange collisions can then couple the Cs and Rb polarizations (as was observed for different ground state hyperfine levels of ^{85}Rb in Ref. [64]). This is significant, since in our studies of NMOR employing the light-polarization modulation technique, we found that the optimum sensitivity occurred for

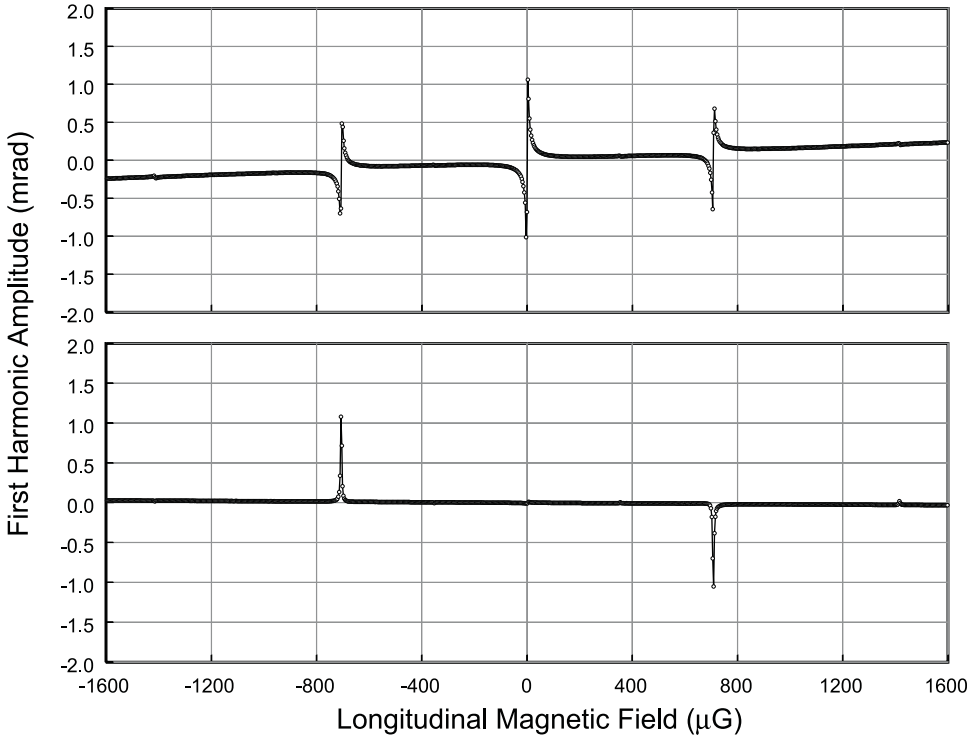

FIGURE 15. FM NMOR signals detected at the first harmonic of Ω_m as a function of longitudinal magnetic field. The laser power was 15 μW, beam diameter $\sim$ 2 mm, $\Omega_m = 2\pi \times 1$ kHz, $\Delta\omega = 2\pi \times$ 220 MHz. Upper plot is the in-phase component (in-phase with the zero-field resonance) and the lower trace is quadrature component from the lock-in output. All resonances have widths corresponding to the slow rate of atomic polarization relaxation in the paraffin-coated cell.

conditions where AOC played an important role [26, 29]. We are presently investigating the role of AOC in FM NMOR.

ATOMS IN CELLS WITH COLD BUFFER GAS

As mentioned above, at the core of the considered experiments is the ability to obtain narrow ($\sim$ 1 Hz) atomic resonances due to the long lifetime of the ground state atomic polarization in an anti-relaxation coated cell [20, 24, 26]. An alternative method of linewidth reduction uses a buffer gas to decrease the rate of depolarizing collisions of atoms with cell walls (see, e.g. [65, 66, 67, 68] and references therein). Recently, with neon as the buffer gas, coherent dark resonances with linewidths as narrow as 42 Hz in cesium [69] and 30 Hz in rubidium [70] were observed in vapor cells at room temperature.

In order to obtain ultra-narrow resonances with sub-Hz width, we are exploring an extension of a buffer-gas method which relies on the properties of atomic scattering at low (cryogenic) temperatures, approaching the S-wave scattering regime, where spin relaxation should be suppressed. Theoretical estimates done in our group suggest that

for the Cs-He case, a significant reduction of the relaxation cross-section, by a factor of $\sim 20-50$, may be expected already at liquid-Nitrogen temperatures.[4] These estimates were confirmed by Prof. Thad Walker of the University of Wisconsin, Madison [71]. Recently, it has been shown experimentally [45] that at temperatures below approximately 2 K, the spin relaxation cross-section of rubidium atoms in collisions with helium buffer gas atoms decrease by orders of magnitude in comparison with their room temperature values. It can be inferred from the data presented in Ref. [45] that relaxation times of minutes (corresponding to resonance widths on the order of 10 mHz) or even longer can be obtained.

The crucial experimental challenge is creating, in the cold buffer gas, atomic vapor densities comparable to those in our current room temperature experiments, i.e. of the order of $10^{10}-10^{12}$ atoms/cm^3. A group in Japan [45] relies on light-induced desorption of alkali atoms from the surface of the liquid He film inside their cell (presumably, this is similar to the effect observed in paraffin coated cells [36]). They can successfully inject Rb atoms into the He gas by irradiating the cell with about 200 mW of Ti:sapphire laser radiation (750 nm) for 10 s. But it turns out that the injection efficiency decreases with the repetitions of the injection cycle. It was found that the efficiency recovered by heating the cell to room temperature and then cooling again. They also report [72] that with their method they cannot inject Cs atoms, which are of particular interest among the alkali atoms for fundamental symmetry tests.

Our method for injecting atoms into the buffer gas differs significantly from that of [45, 72]. We plan to use laser evaporation of micron-sized droplets inside the cold He gas. The central elements of our experimental apparatus consist of: a small cryostat with optical access to the atomic sample (temperature range down to 1.4 K); a droplet generator - a system for injecting micron-size metal droplets into the cold He gas; and a system of lasers for evaporation of these droplets and for optical pumping and probing of the spin relaxation.

The design of the droplet generator is motivated by the “drop-on-demand" liquid micro-droplet generator concept [73] developed by the SLAC group of Prof. Martin Perl for their experiment searching for elementary particles with fractional electric charge [74, 75, 76, 77, 78]. However, the implementation of this method is restricted to elements whose melting point lies below the operational temperature of the dropper's piezo-ceramic transducer (the Curie temperature for some special piezo-ceramics can reach $\sim 360^\circ$C). Fortunately, cesium (melting point of 29°C [79]) is one such element. We have recently proposed the extension of the method to the elements for which fine powders are available (such as Ag and Au). The idea is to load the dropper with powder and produce powder particles with the similar way as liquid drops. Preliminary experiments with a SLAC glass dropper (100 μm orifice diameter) and spherical silver powder with maximum size of ~ 20 μm (635 mesh) have shown generation of the powder clots with rather stable size (comparable with the dropper orifice diameter [80]).

Once the drop has reached the interaction region, it will be heated and vaporized by a sequence of two pulses from a 1-micron wavelength YAG laser. Estimates show that a

[4] Our estimates of low temperature dependence of Cs electron spin relaxation cross-section due to the spin-rotation interaction with He atoms are based on the approach developed in Ref. [67].

500 mJ, 10 ns (2 mm beam diameter) initial pulse will cause the droplet to explode into a collection of small clusters [81], and a subsequent pulse will evaporate these clusters, creating a dense atomic vapor in the He buffer gas. Large residual drops will quickly fall from the interaction region.

In the first stage of the experiment, we plan to investigate spin-relaxation processes of polarized silver atoms in He buffer gas using the relaxation in the dark method [37]. The injected atoms will be optically pumped with a silver hollow cathode lamp into a spin-polarized state, and the atomic vapor polarization will decay in the holding magnetic field created by coils outside the cryostat. After a period of evolution in the dark, the polarization will be optically probed, from which we will deduce the spin-relaxation lifetime and cross-section.

If the Ag-He spin relaxation cross section is as small as expected at low temperatures, then it will be possible to obtain spin-polarized atomic vapors with lifetimes of the order of minutes. The corresponding resonance widths will thus be on the order of mHz. Such narrow resonances may be applied to atomic tests of discrete symmetries, such as a search for the electron EDM. (Silver atoms have an EDM enhancement factor of ~ 50 [82], which is only a factor of two smaller than that for Cs ~ 120 [53, 54, 55, 56]. For gold atoms, the enhancement factor is even larger: ~ 250 [83, 84]). Narrow resonances may also be used for very sensitive measurements of magnetic fields. This method is being considered for detection of the electric-field-induced P,T-odd magnetization of a bulk ferro-magnetic material at low, ~ 50 mK, temperatures [85]. (An experiment of this type was first proposed by F. L. Shapiro in 1968 [86] and carried out by B. V. Vasiliev and E. V. Kolycheva in the end of the 1970's [87].)

TESTING PARITY CONSERVATION AND TIME-REVERSAL-INVARIANCE OF GRAVITY

Finally we would like to mention that nonlinear optical rotation can be used for other types of fundamental symmetry tests. For example, one idea that has been the subject of a few lunch-time conversations with Professor Commins is an experimental test of the symmetry properties of gravity. Gravity is by far the weakest and, it could be argued, least understood of the known fundamental interactions. Many authors have considered the possibility that gravity may violate parity and time-reversal invariance [88, 89, 90, 91, 92, 93]. In the nonrelativistic limit, the simplest Hamiltonian $H_{\rm G}$ describing such an interaction is given by

$$H_{\rm G} = k\frac{\hbar}{c}\vec{g}\cdot\vec{S}, \tag{11}$$

where k is a dimensionless constant specifying the strength of the new interaction, $\vec{g}$ is the gravitational field due to, e.g., the earth, and $\vec{S}$ is the total spin of the system. The energy shift due to the interaction of an atom with the Earth is $\approx k\cdot(2\times10^{-23}$ eV), corresponding to a frequency shift of $\approx k\cdot(4\times10^{-9}$ Hz).

Presently, the most sensitive search for a long-range P- and T-violating gravitational interaction was performed by measuring the nuclear spin-precession frequencies of ^{199}Hg and ^{201}Hg as the direction of an applied magnetic field was reversed with respect

to the earth's gravitational field [94] – this approach is similar to that employed in the Hg EDM experiments (see Ref. [95] and Refs. therein), except that the electric field is replaced by the earth's gravitational field. This experiment set a limit of $k < 70$.

An experiment employing nonlinear optical rotation appears capable of probing the particularly interesting region of $k \lesssim 1$. Consider, for example, an experiment measuring the precession frequencies of Cs atoms in the $F = 3$ and $F = 4$ ground state hyperfine levels,[5] for which $g_F \approx -1/4$ and $+1/4$, respectively. (Note that in such a measurement, corrections to the Landé factors due to the presence of a nonzero magnetic field must be taken into account.) The precession frequencies can be measured for different orientations of the magnetic field with respect to $\vec{g}$ using, e.g., the FM NMOR technique. The precession frequencies $\Omega_p(\pm)$ for the two ground state hyperfine levels in the presence of a magnetic field $\vec{B}$ along the direction of $\vec{g}$ are given by

$$\Omega_p(\pm) = \frac{k\hbar g}{c} \pm |g_F|\mu_B B. \tag{12}$$

We can then take the ratio of the two precession frequencies:

$$\frac{\Omega_p(+)}{\Omega_p(-)} \approx 2\frac{k\hbar g}{c|g_F|\mu_B B} - 1, \tag{13}$$

which constitutes a measurement of k.

The sensitivity of NMOR in paraffin coated cells ($\sim 10^{-6}$ Hz$/\sqrt{\text{Hz}}$), and, potentially, in cells filled with cryogenic buffer gas, offer a possibility of probing $k \lesssim 1$.

CONCLUSION

In conclusion, we have discussed nonlinear optical rotation of linearly polarized light related to the evolution of light-induced atomic polarization in magnetic and electric fields. In certain systems, such as atomic vapor cells coated with paraffin or filled with cold buffer gas, the relaxation rate of atomic polarization can be made very slow ($\lesssim 1$ Hz). Using these techniques, the sensitivity to Zeeman sublevel shifts is $\lesssim 10^{-6}$ Hz$/\sqrt{\text{Hz}}$, permitting a variety of atomic tests of fundamental symmetries. Hopefully, we can follow in Professor Commins's footsteps and bring these ideas to fruition!

ACKNOWLEDGMENTS

We would like to sincerely thank our collaborators in St. Petersburg, Russia, E. B. Alexandrov and M. V. Balabas, for providing us with the paraffin-coated vapor cells; L. Zimmerman and K. Kerner for assistance with some of the described experiments; D. DeMille, L. Hunter, and M. Romalis for fruitful discussions; A. Vaynberg, S. Bonilla, S. Butler, M. Solarz, and G. Weber for excellent machining of various

[5] For the ground states of alkali atoms $\vec{F} = \vec{S}$.

parts of the apparatus; and J. R. Davis for invaluable assistance with the electronics. We would like to thank Professor Commins for inspiration and many useful discussions.

REFERENCES

1. S. A. Murthy, D. Krause, Jr., Z. L. Li, and L. R. Hunter, Phys. Rev. Lett. **63**, 965 (1989).
2. K. Abdullah, C. Carlberg, E. D. Commins, H. Gould, and S. B. Ross, Phys. Rev. Lett. **65**, 2347 (1990).
3. C. Chin, V. Leiber, V. Vuletić, A. J. Kerman, and S. Chu, Phys. Rev. A **63**, 033401 (2001).
4. D. DeMille, F. Bay, S. Bickman, D. Kawall, D. Krause, Jr., S. E. Maxwell, and L. R. Hunter, Phys. Rev. A **61**, 052507 (2000); D. DeMille, in these Proceedings.
5. E. D. Commins, S. B. Ross, D. DeMille, and B. C. Regan, Phys. Rev. A **50**, 2960 (1994).
6. B. C. Regan, E. D. Commins, C. J. Schmidt, and D. DeMille, "New limit on the electron electric dipole moment," (to be published).
7. M. Faraday, *Experimental Research* **III** (London), 2164 (1855).
8. D. Macaluso and O. M. Corbino, Nuovo Cimento **8**, 257 (1898).
9. N.B. Baranova, Yu. V. Bogdanov, and B. Ya. Zel'dovich, Usp. Fiz. Nauk. **122-123**, 349 (1977) [Sov. Phys. Usp. **20**, 870 (1977)].
10. O.P. Sushkov and V.V. Flambaum, Zh. Eksp. Teor. Fiz. **75**, 1208 (1978) [Sov. JETP **48**, 608 (1978)].
11. Note, however, that with squeezed states of light the sensitivity to polarization rotation can in principle surpass the shot-noise-limit: see, e.g., P. Grangier, R.E. Slusher, B. Yurke and A. LaPorta, Phys. Rev. Lett. **59**, 2153 (1987).
12. W. Gawlik, in *Modern Nonlinear Optics* edited by M. Evans and S. Kielich, Advances in Chemical Physics Series, Vol. **LXXXV**, Pt. 3 (Wiley, New York, 1994).
13. D. Budker, D. J. Orlando, and V. Yashchuk, Am. J. Phys. **67**, (1999); D. Budker, V. Yashchuk, and M. Zolotorev, Sib. J. Phys. **1**, 27 (1999).
14. W.R. Bennett, Phys. Rev. **126**, 580 (1962).
15. L. M. Barkov, D. Melik-Pashayev, and M. Zolotorev, Opt. Commun. **70**, 467 (1989).
16. A detailed description of this density matrix calculation can found in S.M. Rochester, D.S. Hsiung, D. Budker, R.Y. Chiao, D.F. Kimball, and V.V. Yashchuk, Phys. Rev. A **63**, 043814 (2001).
17. D. Budker, D. F. Kimball, S. M. Rochester, and V. V. Yashchuk, "Nonlinear electro- and magneto-optic effects related to Bennett structures," (to be published).
18. S. I. Kanorsky, A. Weis, J. Wurster, and T. W. Hänsch, Phys. Rev. A **47**, 1220 (1993).
19. A. Weis, J. Wurster, and S. I. Kanorsky, J. Opt. Soc. Am. B **10**, 716 (1993).
20. D. Budker, V. Yashchuk, and M. Zolotorev, Phys. Rev. Lett. **81**, 5788 (1998).
21. H.G. Robinson, E.S. Ensberg, and H.G. Dehmelt, Bull. Am. Phys. Soc. **3**, 9 (1958).
22. M. A. Bouchiat and J. Brossel, Phys. Rev. **147**, 41 (1966).
23. E. B. Alexandrov and V. A. Bonch-Bruevich, Opt. Engin. **31**, 711 (1992).
24. V. Yashchuk, D. Budker and M. Zolotorev, in *Trapped Charged Particles and Fundamental Physics*, edited by D.H.E. Dubin and D. Schneider (American Institute of Physics, New York, 1999), pp. 177-181.
25. S. M. Rochester and D. Budker, Am. J. Phys. **69**, 450 (2001).
26. D. Budker, D. F. Kimball, S. M. Rochester, V. V. Yashchuk, and M. Zolotorev, Phys. Rev. A **62**, 043403 (2000).
27. E.B. Alexandrov, M.V. Balabas, A.S. Pasgalev, A.K. Vershovskii, and N.N. Yakobson, Laser Phys. **6**, 244 (1996).
28. J. Clarke in *The New Superconducting Electronics*, edited by H. Weinstock and R.W. Ralston, pp. 123-180 (Kluwer Academic, The Netherlands, 1993).
29. D. Budker, D. F. Kimball, S. M. Rochester, and V. V. Yashchuk, Phys. Rev. Lett. **85**, 2088 (2000).
30. M. Lombardi, J. Physique **30**, 631 (1969).
31. C. Cohen-Tannoudji and J. Dupont-Roc, Opt. Commun. **1**, 184 (1969).
32. M. Pinard and C.G. Aminoff, J. Physique **43**, 1327 (1982).
33. R.C. Hilborn, L.R. Hunter, K. Johnson, S.K. Peck, A. Spencer, and J. Watson, Phys. Rev. A **50**, 2467 (1994).

34. R.C. Hilborn, Am. J. Phys. **63**, 330 (1995).
35. M.V. Balabas, V.A. Bonch-Bruevich, and S.V. Provotorov, in *Proceedings of the First All-Union Seminar on Quantum Magnetometers* (S.I. Vavilov State Univ. Press, Leningrad, 1988), pp. 55-56.
36. E. B. Alexandrov, M. V. Balabas, D. Budker, D. S. English, D. F. Kimball, C.-H. Li, and V. V. Yashchuk, "Light-induced desorption of alkali atoms from paraffin coating," (to be published).
37. W. Franzen, Phys. Rev. **115**, 850 (1959).
38. G.N. Birich, Yu.V. Bogdanov, S.I. Kanorskii, I.I. Sobelman, V.N. Sorokin, I.I. Struk, and E.A. Yukov, J. of Russian Laser Research, **15**, 455 (1994).
39. I. N. Abramova, E. B. Aleksandrov, A. M. Bonch-Bruevich, and V. V. Khromov, Pis'ma Zh. Eskp. Teor. Fiz. **39**, 172 (1984) [JETP Lett. **39**, 203 (1984)].
40. A. Gozzini, F. Mango, J. H. Xu, G. Alzetta, F. Maccarrone, and R. A. Bernheim, Nuovo Cimento D **15**, 709 (1993).
41. M. Meucci, E. Mariotti, P. Bicchi, C. Marinelli, and L. Moi, Europhys. Lett. **25**, 639 (1994).
42. E. Mariotti, S. Atutov, M. Meucci, P. Bicchi, C. Marinelli, and L. Moi, Chem. Phys. **187**, 111 (1994).
43. J. H. Xu, A. Gozzini, F. Mango, G. Alzetta, and R. A. Bernheim, Phys. Rev. A **54**, 3146 (1996).
44. S. Atutov, V. Biancalana, P. Bicchi, C. Marinelli, E. Mariotti, M. Meucci, A. Nagel, K. A. Nasyrov, S. Rachini, and L. Moi, Phys. Rev. A **60**, 4693 (1999).
45. A. Hatakeyama, K. Oe, K. Ota, S. Hara, J. Arai, T. Yabuzaki, and A.R. Young, Phys. Rev. Lett. **84**, 1407 (2000).
46. I. B. Khriplovich and S. K. Lamoreaux, *CP Violation Without Strangeness: Electric Dipole Moments of Particles, Atoms, and Molecules* (Springer-Verlag, Berlin, 1997).
47. E. N. Fortson, in these Proccedings.
48. L. M. Barkov, M. S. Zolotorev and D. Melik-Pashayev, Sov. JETP Pis'ma **48**, 144 (1988).
49. E. S. Ensberg, Bull. Am. Phys. Soc. **7**, 534 (1962).
50. E. S. Ensberg, Phys. Rev. **153**, 36 (1967).
51. P. A. Ekstrom, Ph.D. Thesis (University of Washington, Seattle, 1971).
52. H. G. Dehmelt, Phys. Rev. **105**, 1924 (1957).
53. P.G.H. Sandars, Phys. Lett. **22**, 290 (1966).
54. W.R. Johnson, D.S. Guo, M. Idrees, and J. Sapirstein, Phys. Rev. A **34**, 1043 (1986).
55. B.P. Das, *Recent Advances in Many Body Theory* (Springer-Verlag, New York, 1988).
56. A. C. Hartley, E. Lindroth, and A.-M. Martensson-Pendrill, J. Phys. B **23**, 3417 (1990).
57. D. Budker, D. F. Kimball, S. M. Rochester, and V. V. Yashchuk, LBNL Preprint PUB5453 (Berkeley, CA, 1999).
58. K. Green, P. G. Harris, P. Iaydjiev, D. J. R. May, J. M. Pendlebury, K. F. Smith, M. van der Grinten, P. Geltenbort, and S. Ivanov, Nucl. Instr. and Meth. A **404**, 381 (1998).
59. I. S. Girgoriev and E. Z. Meilikhov, eds., *Handbook of Physical Quantities* (CRC Press, Boca Raton, FL, 1997).
60. H. G. Gibbs and R. J. Hull, Phys. Rev. **153**, 132 (1967).
61. S. Haroche and C. Cohen-Tannoudji, Phys. Rev. Lett. **24**, 974 (1970).
62. H. Ito, T. Ito, and T. Yabuzaki, J. Phys. Soc. Jpn. **63**, 1337 (1994); T. Ito, N. Shimomura, and T. Yabuzaki, J. Phys. Soc. Jpn. **64**, 2848 (1995).
63. D. Budker, D.F. Kimball, V.V. Yashchuk, and M. Zolotorev, "Nonlinear magneto-optical rotation with frequency-modulated light," (to be published).
64. V. V. Yashchuk, E. Mikhailov, I. Novikova, and D. Budker, "Nonlinear magneto-optical rotation with separated light fields in ^{85}Rb vapor contained in an antirelaxation-coated cell," Preprint LBNL-44762 (1999).
65. W. Happer, Rev. Mod. Phys. **44**, 169 (1972).
66. J. Vanier and C. Audoin, *The Quantum Physics of Atomic Frequency Standards, vol.* **1** (Adam Hilger, Bristol and Filadelfia, 1989).
67. T. G. Walker, J. H. Thywissen, and W. Happer, Phys. Rev. A **56**, 2090 (1997).
68. D. K. Walter, W. Happer, and T. G. Walker, Phys. Rev. A **58**, 3642 (1998).
69. S. Brandt, A. Nagel, R. Wynands, and D. Meschede, Phys. Rev. A **56**, R1063 (1997).
70. M. Erhard, S. Numann, and H. Helm, Phys. Rev. A **62**, 061802(R) (2000).
71. T. G. Walker, private communication, March, 2001.
72. A. Hatakeyama, K. Enomoto, and T. Yabuzaki, in *ICAP 2000 (XVII International Conference on Atomic Physics, Firenze, Italy, June 4-9, 2000), Conference Abstracts*, (Universita di Firenze, 2000),

p.557.
73. D. Loomba, V. Halyo, E.R. Lee, I.T. Lee, P. C. Kim, and M. L. Perl, Rev. Scient. Instrum. **71**, 3409 (2000).
74. N. M. Mar, E. R. Lee, G. R. Fleming, B. C. K. Casey, M. L. Perl, E. L. Garwin, C. D. Hendricks, K. S. Lackner, and G. L. Shaw, Phys. Rev. D **53**, 6017 (1996).
75. M. L. Perl, E. R. Lee, Am. J. Phys. **65**, 698 (1997).
76. V. Halyo, P. C. Kim, E.R. Lee, I.T. Lee, D. Loomba, and M. L. Perl, Phys. Rev. Lett. **84**, 2576 (2000).
77. M. L. Perl, P. C. Kim, V. Halyo, E.R. Lee, I.T. Lee, D. Loomba, and K. S. Lackner, Int. J. of Modern Physics A **16**, 2137 (2001).
78. M. L. Perl, in these Proceedings.
79. C. C. Addison, *The chemistry of the liquid alkali metals* (John Wiley & Sons, New York, 1984).
80. V. V. Yashchuk, A. O. Sushkov, D. Budker, E.R. Lee, I.T. Lee, and M. L. Perl, to be published.
81. R. L. Armstrong, in *Optical effects associated with small particles. Edited by P.W.Barber, R.K.Chang.* (World Scientific, Singapore, 1988), p.p. 200-275.
82. Our estimate is based on the expression for the EDM enhancement factor given in I. B. Khriplovich, *Parity Nonconservation in Atomic Phenomena* (Gordon and Breach, Philadelphia, 1991).
83. W. R. Johnson, D. S. Guo, M. Idrees, J. Sapirstein, Phys. Rev. A **34**, 1043 (1986).
84. T. M. R. Byrnes, V. A. Dzuba, V. V. Flambaum, and D. W. Murray, Phys. Rev. A **59**, 3082 (1999).
85. S. K. Lamoreaux, private communication, July, 2001.
86. F. L. Shapiro, Usp. Fiz. Nauk **95**,145 (1968) [Sov. Phys. Uspekhi **11**, 345 (1968)].
87. B. V. Vasiliev and E. V. Kolycheva, Zh. Eskp. Teor. Fiz. **74**, 466 (1978) [Sov. Phys. JETP **74**, 466 (1978)].
88. I. Y. Kobzarev and L. B. Okun, Zh. Eskp. Teor. Fiz. **43**, 1904 (1962) [Sov. Phys. JETP **16**, 1343 (1963)].
89. T. A. Morgan and A. Peres, Phys. Rev. Lett. **9**, 79 (1962).
90. J. Leitner and S. Okubo, Phys. Rev. **136**, B 1542 (1964).
91. N.D. Hari Dass, Phys. Rev. Lett. **36**, 393 (1976).
92. W. T. Ni, Phys. Rev. Lett. **38**, 301 (1977).
93. Y. N. Obukhov, Phys. Rev. Lett. **86**, 192 (2001).
94. B. J. Venema, P. K. Majumder, S. K. Lamoreaux, B. R. Heckel, and E. N. Fortson, Phys. Rev. Lett. **68**, 135 (1992).
95. M. V. Romalis, W. C. Griffith, J. P. Jacobs, and E. N. Fortson, Phys. Rev. Lett. **86**, 2505 (2001); M. V. Romalis, in these Proceedings.